BULLETIN OF THE POLISH ACADEMY OF SCIENCES
TECHNICAL SCIENCES, Vol. 64, No. 3, 2016
DOI: 10.1515/bpasts-2016-0062

Facile preparation of copper impregnated aluminum pillared montmorillonite: nanoclays for wastewater treatment

P. TEPMATEE[1] and P. SIRIPHANNON[1,2]*

[1]Functional Nanostructured Materials Laboratory, College of Nanotechnology, King Mongkut's Institute of Technology Ladkrabang, Chalongkrung Road, Ladkrabang, Bangkok 10520, Thailand

[2]Department of Chemistry, Faculty of Science, King Mongkut's Institute of Technology Ladkrabang, Chalongkrung Road, Ladkrabang, Bangkok 10520, Thailand

Abstract. Copper impregnated aluminum pillared montmorillonites (Cu-iAlpill-MMTs) were prepared by adding Cu^{2+} solution into dried aluminum polyohydroxy cation intercalated montmorillonite using various Cu^{2+} concentrations, i.e. 4, 7, 10 and 13 wt% and then calcining at 500ºC. The Cu-iAlpill-MMTs possessed slit-liked mesopores with pore diameters of 3.3–3.8 nm and ~6–35 nm as observed from the nitrogen adsorption isotherms. The mesopore quantities of Cu-iAlpill-MMTs gradually decreased with the increase of impregnated Cu^{2+} concentrations. The impregnated CuO occupied not only the interior interlayers, but also the exterior surfaces of Cu-iAlpill-MMTs. The Cu-iAlpill-MMTs with 10 and 13 wt% of impregnated Cu^{2+} could inhibit the growth of *Escherichia coli*. The Cu-iAlpill-MMTs effectively acted as the heterogeneous catalyst for removal reactive orange 16 (RO16) in Fenton or photo-Fenton oxidation treatments. The higher impregnated Cu^{2+} and/or the longer treatment time brought about the higher percentage of RO16 removal.

Key words: pillared montmorillonite, mesoporous materials, impregnation, advanced oxidation processes, adsorption.

1. Introduction

Aluminum pillared clays have been considered as adsorbents and catalysts, especially in environmental applications due to their high acidic property, high surface area and porosity, thermal stability, reusability and low cost [1–3]. They are commonly obtained by intercalation of aluminum polyhydroxy cation in the interlayer of clays and followed by calcinations [4–5]. In addition, some research works have modified the aluminum pillared clays by doping the transition metals, such as Cr, Ag, V, Fe, Mn, Ti, Ce, Pd, Cu, etc., in order to create the active sites for the catalysis reactions [6–7]. Among various transition metals, the copper (Cu) have attracted considerable attention as the dopant because it could induce the catalytic oxidation *via* Fenton and photo-Fenton reactions [8], resulting in the degradation of various organic pollutants, such as synthetic dyes [9–11], phenol [12], olive oil mill [13], agro food [14], etc. Besides, the Cu dopant could also inhibit bacterial growth, indicating its antibacterial property [15–16].

From the attractive properties of Cu dopant, our previous work prepared the Cu doped aluminum pillared montmorillonite by sonication process [17]. The Cu doped aluminum pillared montmorillonite acted as the heterogeneous catalyst for effective removal the reactive dye, however, the quantity amount of doped Cu in the pillared structure could not be exactly controlled in the sonication process. Therefore, the present work aimed to prepare the Cu doped aluminum pillared montmorillonite using facile impregnation method, in which the Cu doped amount was controllable. The Cu impregnation was performed using the aluminum polyhydroxy cation intercalated montmorillonite as the host substrate since the intercalated aluminum polyhydroxy cation could enlarge the interlayer space of montmorillonite, resulting in the increase of impregnated Cu uptake. In addition, the concentration of impregnated Cu was varied in order to investigate its effect on the structure and properties of the resultant products since the Cu quantity was considered to play an important role in the catalytic activity and antibacterial property.

The catalytic oxidation activities of the as-prepared Cu impregnated aluminum pillared montmorillonites were investigated for removal reactive orange 16 (RO16). This reactive dye was used as a model dye containing wastewater because it was commonly used in textile industries due to its easy application in dyeing process and stability during usage [18]. However, the stability of reactive dyes resulted in the difficulty in elimination by biological and conventional wastewater treatments, therefore; the reactive dyes were important pollutants from the textile effluents. The as-prepared Cu impregnated aluminum pillared montmorillonites were considered to promote the decolourisation, degradation and mineralisation of reactive dye from the model wastewater.

2. Experiment

2.1. Materials. Sodium montmorillonite (Na^+-MMT) with the cation exchange capacity of about 1.0 meq/g was supported

*e-mail: punnama.si@kmitl.ac.th

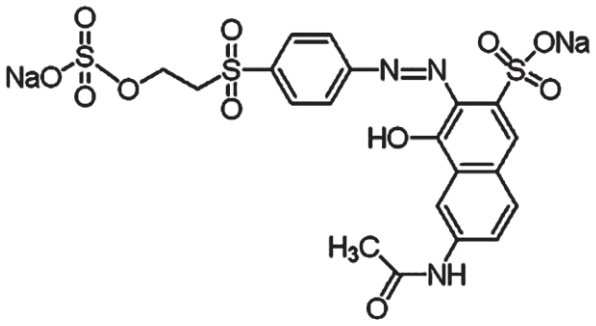

Fig. 1. Chemical structure of reactive orange 16

from Thai Nippon Chemical Industry Co., Ltd. (Thailand). The Na^+-MMT was purified to remove some contaminants by dispersion and sonication in distilled water for 10 min. The upper layer of swollen Na^+-MMT suspension was decanted and dried at 100°C for 24 hours. Aluminum nitrate nonahydrate ($Al(NO_3)_3 \cdot 9H_2O$, 98%) was purchased from Rankem. Copper (II) sulfate pentahydrate ($CuSO_4 \cdot 5H_2O$, 98%) and sodium hydroxide (NaOH, 97%) were purchased from Carlo Erba.

Reactive Orange 16 (RO16, dye content 70%) was purchased from Sigma Aldrich, whose structure was shown in Fig. 1. Hydrogen peroxide (H_2O_2, 35% v/v) was purchased from *QRëC* chemical.

2.2. Preparation of copper impregnated aluminum pillared montmorillonites. An aluminum polyhydroxy cation solution (AlOH) with OH/Al molar ratio of 2.4 was obtained by mixing 0.4 M NaOH and 0.4 M $Al(NO_3)_3 \cdot 9H_2O$ with continuous stirring for 3 hours at 60°C and then aged overnight at room temperature. The prepared AlOH solution was slowly added into an aqueous Na^+-MMT suspension with vigorous stirring. The ratio of mmol-Al^{3+}/g-Na^+-MMT used in the intercalation process was fixed at 2.5. After 24-hour mixing, the mixture suspension was filtered, washed several times with distilled water and dried overnight at 100°C in order to obtain the AlOH intercalated Na^+-MMT (AlOH-MMT). The AlOH-MMT was impregnated with the $CuSO_4 \cdot 5H_2O$ aqueous solution having various concentration of Cu^{2+}, i.e. 4, 7, 11 and 13 wt% of AlOH-MMT. The impregnated products were dried overnight at 100°C and calcined at 500°C for 2 hours in order to obtain the copper impregnated aluminum pillared MMTs (Cu-iAlpill-MMTs).

The starting Na^+-MMT, AlOH-MMT and Cu-iAlpill-MMTs samples were characterized by X-ray fluorescence spectrometer (XRF; Bruker AG, SRS3400) and X-ray diffractometer (XRD; Bruker AG, D8 ADVANCE) in order to determine their chemical compositions and crystalline structure, respectively. Nitrogen adsorption isotherms of starting Na^+-MMT and the Cu-iAlpill-MMTs were performed at –196°C using Quantachrome Autosorb 1 for determination of their specific surface areas (SSA), pore volumes and pore size distributions. Prior to evaluating the nitrogen adsorption, all samples were outgassed at 300°C for 3 hours. Surface morphologies of the Cu-iAlpill-MMTs were investigated by scanning electron microscope (SEM; JEOL, JSM-5410) and the elemental distribution of copper (Cu) on the Cu-iAlpill-MMTs surfaces was determined by energy dispersive X-ray microanalysis (EDX) incorporated with the SEM.

2.3. Antibacterial activity test. The antibacterial activities of Cu-iAlpill-MMTs were performed according to the JIS L 1902: 1998 (Qualitative) technique using *Escherichia coli* (*E.coli*) ATCC®25922. One gram of Cu-iAlpill-MMTs was shaped by uniaxial pressing into cylindrical pellet with 1.3 ±0.1 cm in diameter. The pellet of Cu-iAlpill-MMTs was placed on the surface of agar plate inoculated with a cell suspension of *E.coli* and then incubated at 37°C for 24 hours. All tests were performed in triplicate according to the standard test method. The size of inhibition zone around the samples was evaluated.

2.4. Determination of dye removal. The Cu-iAlpill-MMTs prepared were used as catalysts for dye removal in Fenton and photo-Fenton systems. An aqueous solution of 300 mg/L RO16 was used as a dye-containing wastewater model.

A. Fenton system. The Fenton treatment was performed by mixing 0.2 g of Cu-iAlpill-MMTs in 20 ml of RO16 solution and 5 ml of 0.1 M hydrogen peroxide (H_2O_2) with continuous stirring. The treatment times was varied, i.e. 60, 120, 240 and 360 min. After predetermined treatment time, the Cu-iAlpill-MMTs were separated from the mixture solution by centrifugation.

B. Photo-Fenton system. In photo-Fenton treatment, the similar mixture of Cu-iAlpill-MMT, RO16 and H_2O_2 as described above was irradiated with 6W UVC-radiation (l = 254 nm; TUV TL Mini, Philips). The mixture was continuously stirred for various reaction times, i.e. 30, 60, 90, 120, 240 and 360 min. After predetermined treatment time, the Cu-iAlpill-MMTs were separated from the mixture solution by centrifugation.

The RO16 solutions before and after Fenton and photo-Fenton treatments were analyzed by UV-visible spectrophotometry (UV-Vis; Thermo scientific, Helios omega) at l_{max} of 388 nm for RO16. The RO16 concentrations in the dye solutions were evaluated by linear regression equation from the standard calibration curve (Y = 0.0064X, R^2 = 0.9999; Y is UV-Vis absorbance and X is final concentration of RO16 in mg/L). Percentage of dye removal was calculated from equation (1):

$$\%\ dye\ removal = \frac{(C_0 - C_f)}{C_0}\ x\ 100\,, \qquad (1)$$

where C_0 and C_f are initial and final concentrations of dye solutions (mg/L), respectively.

Total organic carbon (TOC) values in the RO16 solutions before and after Fenton and photo-Fento treatments were analyzed by TOC analyzer (Shimadzu, TOC-VCPH). Percentage of TOC removal was calculated from equation (2):

$$\%\ TOC\ removal = \frac{(TOC_0 - TOC_f)}{TOC_0}\ x\ 100\,, \qquad (2)$$

where TOC_0 and TOC_f are initial and final TOC of dye solutions (mg/L), respectively.

3. Results and discussion

3.1. Characterization of Cu-iAlpill-MMT. Figure 2 shows the XRD patterns of Cu-iAlpill-MMTs are shown in comparison with the starting Na^+-MMT and the AlOH-MMT precursor. It was found that the interlayer space of starting Na^+-MMT tactoids in Fig. 2a was observed at $2 \approx 7.12°$, corresponding to a *001*-plane basal spacing (d_{001}) of 1.24 nm as reported in Table 1. After intercalation with AlOH solution, the cation exchange between aluminum polyhydroxy cation ($[AlO_4Al_{12}(OH)_{24}(OH_2)_{12}]^{7+}$, Al_{13}^{7+}) obtained from base hydrolyzation of $Al(NO_3)_3 \cdot 9H_2O$ and Na^+ interlayer counter ions brought about the expansion of MMT tactoids' interlayer space with disorder structure as previously discussed elsewhere [5]. It was therefore the d_{001} peak in Fig. 2b was broadened and shifted to $2 \approx 5.1°$, corresponding to d_{001} of 1.74 nm. From the XRF analysis, the increases of Al_2O_3 quantity and Al/Si molar ratio were detected in the AlOH-MMT concomitant with the decrease of Na_2O quantity as shown in Table 1, indicating the successful interaction of aluminum polyhydroxy cation in the interlayer space of MMT.

After Cu^{2+} impregnation into the AlOH-MMT and calcination, the d_{001} peak almost disappeared from the XRD patterns of all Cu-iAlpill-MMTs as shown in Fig. 2 (c–f). These results suggested that the impregnated Cu^{2+} could penetrate into the interlayer space of AlOH-MMT, bringing about the delamination of MMT tactoids. The impregnated Cu^{2+} was calcined to CuO, therefore, the crystalline peak of CuO phase was also observed in the XRD patterns of all Cu-iAlpill-MMTs at $2\theta = 35.5°$. The presence of impregnated CuO in the Cu-iAlpill-MMTs was also detected by the XRF analyses as reported in Table 1. The increases of CuO amount and Cu/Si molar ratio in the Cu-iAlpill-MMTs were in agreement with the Cu^{2+}amount used in the impregnation process.

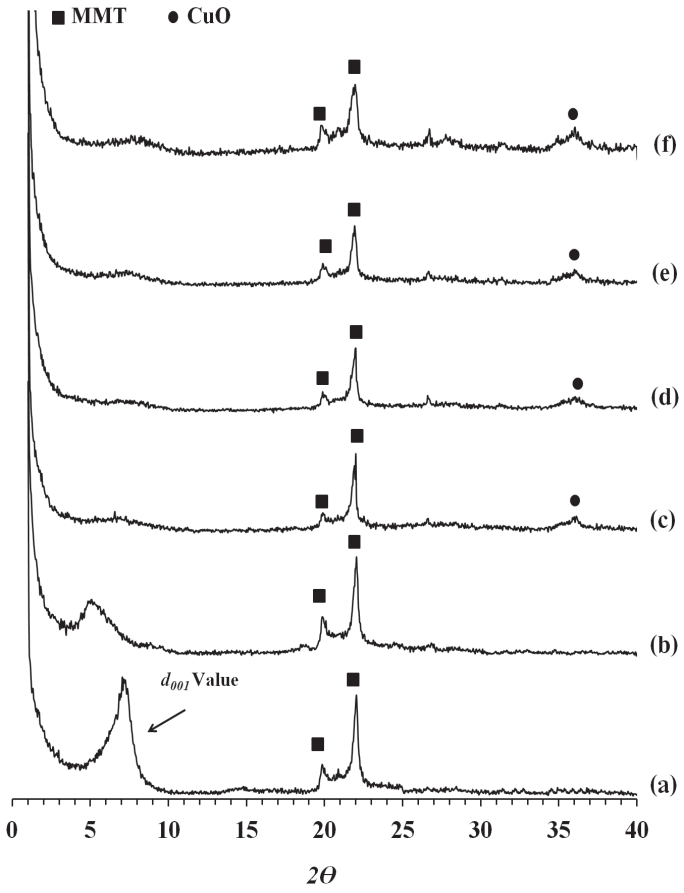

Fig. 2. XRD patterns of (a) Na^+-MMT, (b) AlOH-MMT, (c) Cu-iAlpill--MMT-4wt%, (d) Cu-iAlpill-MMT-7wt%, (e) Cu-iAlpill-MMT-10wt% and (f) Cu-iAlpill-MMT-13wt%

Table 1
Chemical composition, basal spacing (d_{001}), specific surface area (SSA), pore volume and BJH pore diameter of Na^+-MMT, AlOH-MMT and Cu-iAlpill-MMTs

Sample	Chemical composition							Basal spacing	N_2 adsorption		
	Al_2O_3 (wt%)	SiO_2 (wt%)	Na_2O (wt%)	CuO (wt%)	Other (wt%)	Al/Si molar ratio	Cu/Si molar ratio	d_{001} (nm)	SSA (m^2/g)	Pore volume (cm^3/g)	BJH Pore diameter (nm)
Na^+-MMT	11.99	73.44	2.31	0.00	12.26	0.19	n/a	1.24	54	0.20	3.80
AlOH-MMT	18.44	73.68	0.50	0.00	7.38	0.29	n/a	1.74	n/a	n/a	n/a
Cu-iAlpill-MMT-4 wt%	16.17	66.65	0.22	4.92	12.04	0.29	0.06	Broad peak	87	0.19	3.79
Cu-iAlpill-MMT-7 wt%	15.83	61.65	0.23	8.35	13.94	0.30	0.10	Broad peak	40	0.17	3.79
Cu-iAlpill-MMT-10 wt%	14.98	56.23	0.14	12.13	16.52	0.31	0.16	Broad peak	30	0.16	3.79
Cu-iAlpill-MMT-13 wt%	13.95	50.56	0.16	15.40	20.23	0.32	0.23	Broad peak	31	0.06	3.34

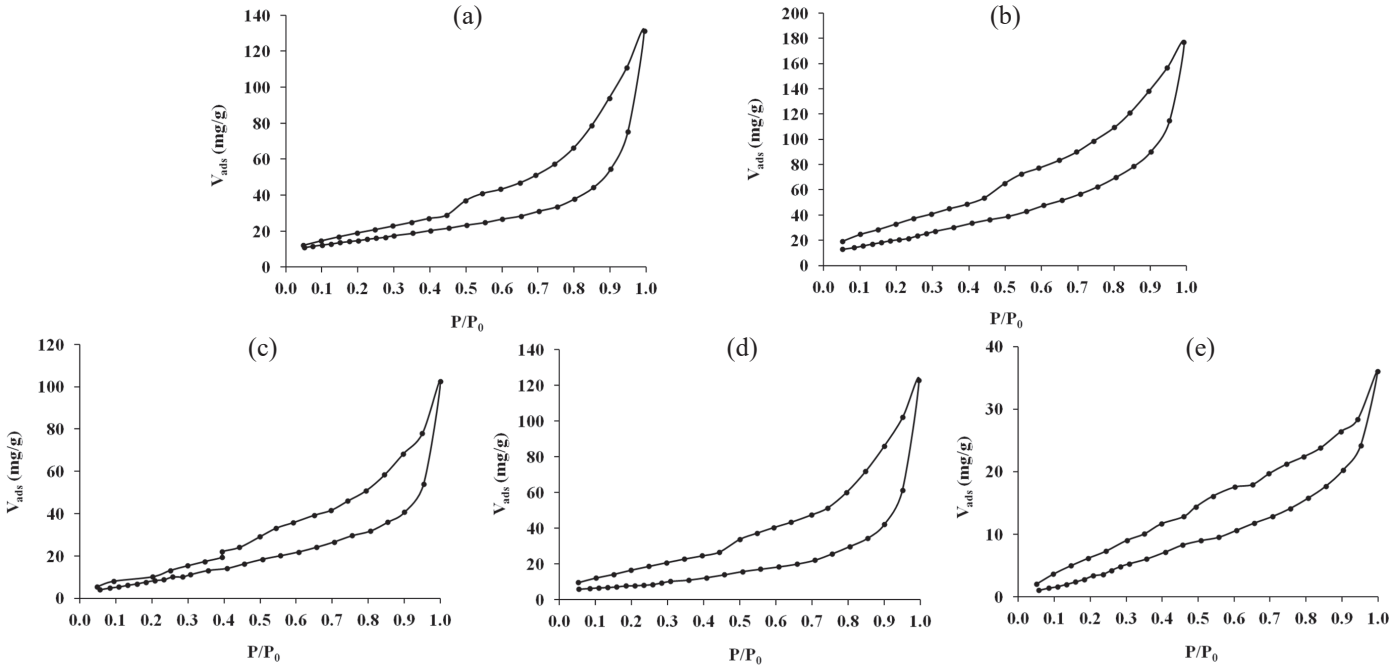

Fig. 3. N2 adsorption isotherms of (a) Na+-MMT, (b) Cu-iAlpill-MMT-4wt%, (c) Cu-iAlpill-MMT-7wt%, (d) Cu-iAlpill-MMT-10wt%, (e) Cu-iAlpill-MMT-13wt%

Figure 3 shows the N_2 adsorption isotherms of the starting Na^+-MMT and all Cu-iAlpill-MMTs. The adsorption isotherms of Na^+-MMT and Cu-iAlpill-MMTs could be classified as type IV isotherm in the Brunauer, Deming, Dewing and Teller (BDDT) classification, having the hysteresis loop of H3 type in IUPAC classification [5]. It was, therefore, indicated that the starting Na^+-MMT and all Cu-iAlpill-MMTs consisted of slit-like mesopore structures (2–50 nm). The Brunaur–Emmet–Teller (BET) equation and Barrett-Joyner-Halenda (BJH) method were respectively used for determination of the SSA and average diameter of mesopores as concluded in Table 1. It was found that the SSA and pore volume of the Cu-iAlpill-MMTs decreased with the increase of the impregnated Cu content. These results were considered to be because the CuO occupied the interior pores of the Cu-iAlpill-MMTs**.** The occupancy of CuO might occur through two main possibilities; i.e. the impregnated Cu^{2+} ions could coordinate to the oxygens of the MMT silicate layer and/or the oxygens of the aluminum polyhydroxy cations intercalated in the AlOH-MMT precursor. Figure 4 shows the BJH pore size distributions of the starting

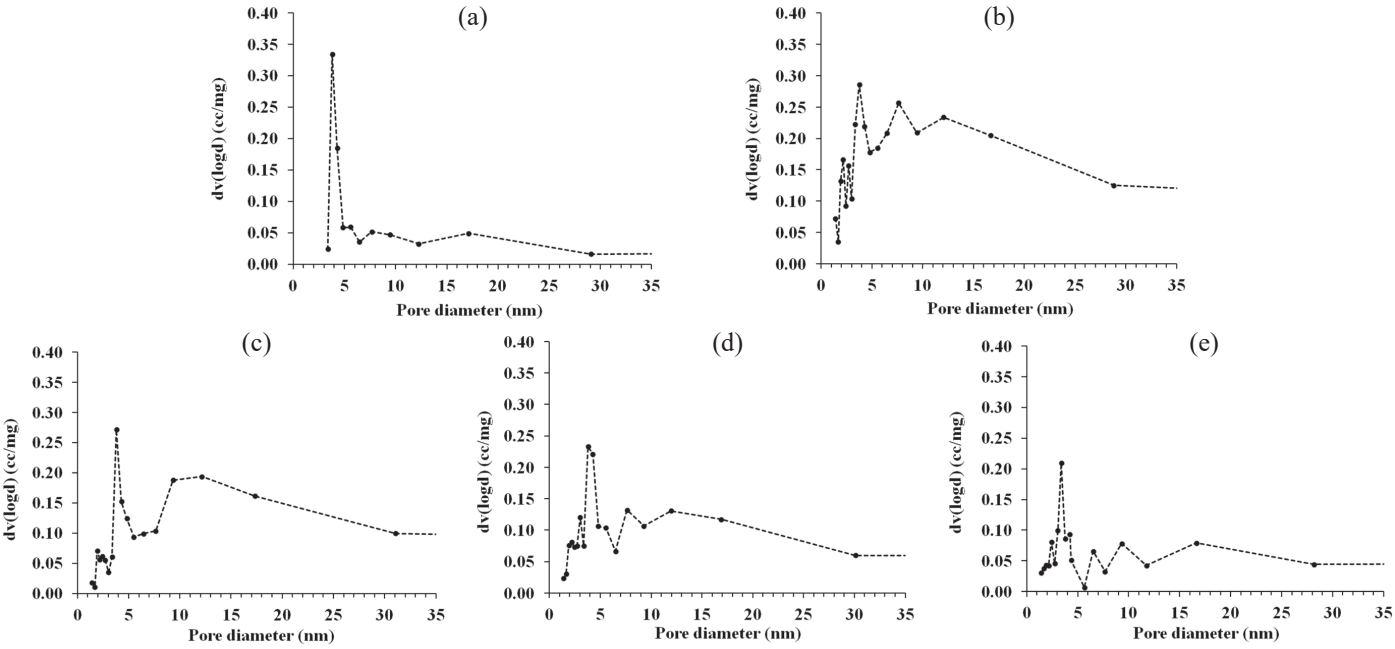

Fig. 4. BJH pore size distributions of (a) Na+-MMT, (b) Cu-iAlpill-MMT-4wt%, (c) Cu-iAlpill-MMT-7wt%, (d) Cu-iAlpill-MMT-10wt%, (e) Cu-iAlpill-MMT-13wt%

Na^+-MMT and all Cu-iAlpill-MMTs. It can be seen that the starting Na^+-MMT possessed the mesopores with average pore diameter of about 3.8 nm as shown in Fig. 4(a). On the other hand, the BJH pore size distributions of all Cu-iAlpill-MMTs have revealed the formation of multiple mesopore sizes ranging from 3.3 to 35 nm in all Cu-iAlpill-MMTs after intercalation and impregnation treatments as observed in Fig. 4b–e. The quantities of mesopores in the Cu-Alpill-MMTs gradually decreased with the increase of the impregnated Cu content due to the pore-filling with CuO.

Figure 5 shows the SEM micrographs of the Cu-iAlpill-MMT surfaces with their Cu mapping images. The regular distribution of Cu was observed on the surfaces of all Cu-iAlpill-MMT samples, suggesting that the impregnated Cu^{2+} ions occupied not only the AlOH-MMT interlayers but also the AlOH-MMT surfaces. The quantity of Cu observed on the EDX mappings of the Cu-iAlpill-MMT surfaces increased with the increase of Cu^{2+}amount used in the impregnation process.

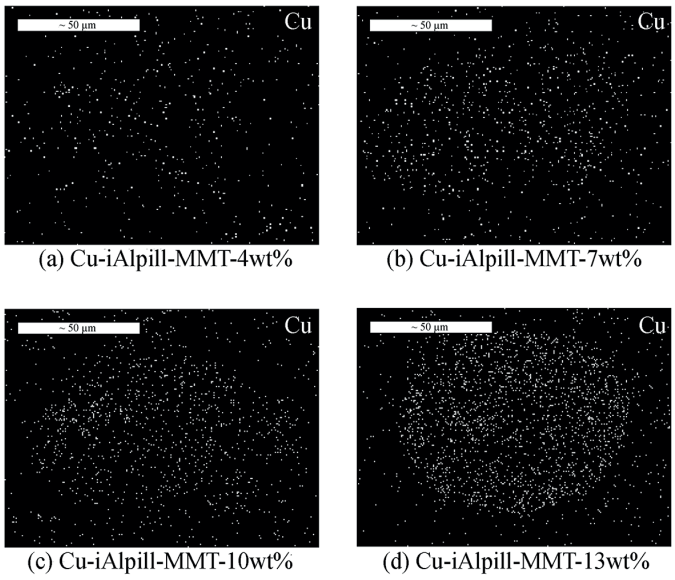

Fig. 5. SEM-EDX Cu mapping images of Cu-iAlpill-MMTs surfaces

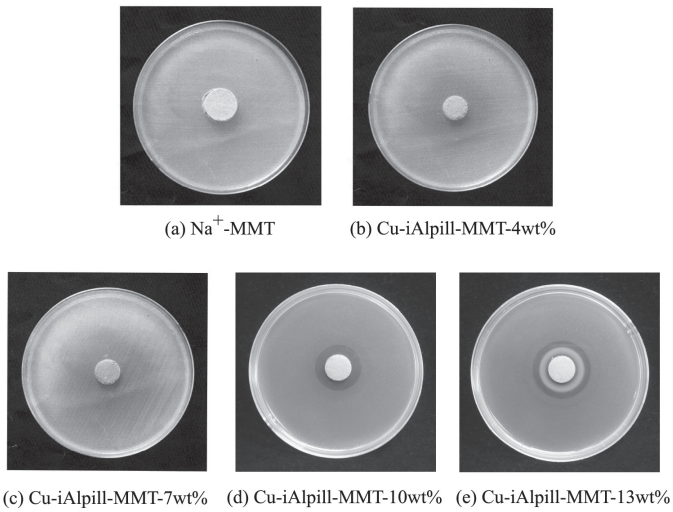

Fig. 6. Antibacterial activities of Na+-MMT and Cu-iAlpill-MMTs for E. coli growth

3.2. Antibacterial activity. Figure 6 shows the antibacterial activities of Cu-iAlpill-MMTs in comparison with the starting Na^+-MMT. It was found that the growth of *E. coli* was observed under the Na^+-MMT, Cu-iAlpill-MMT-4wt% and Cu-iAlpill-MMT-7wt% samples. However, the clear inhibition zones of about 5.5 and 8.5 mm in diameter were obtained under the Cu-iAlpill-MMT-10wt% and Cu-iAlpill-MMT-13wt% samples, respectively. The antibacterial activities of Cu-iAlpill-MMT-10wt% and Cu-iAlpill-MMT-13wt% were attributed to their high impregnated CuO quantities; therefore, they could release the high amount of Cu^{2+} ions. The Cu^{2+} ions could electrostatically interact with the negatively charged *cell* wall of *E. coli*, resulting in death and/or disability in replication of bacteria. In addition, the Cu-iAlpill-MMT-10wt% and Cu-iAlpill-MMT-13wt% were composed of CuO rich surfaces, in which they could generate the reactive oxygen species (ROS) such as $HO^{\bullet-}$, $O_2^{\bullet 2-}$, $HO_2^{\bullet-}$ and H_2O_2 in aqueous suspensions. The ROS further interacted with the *E. coli cell,* destroying the cell integrity [19].

3.3. RO16 removal. The percentages of RO16 removal when using the Cu-iAlpill-MMTs in the Fenton and photo-Fenton systems were summarized in Table 2.

A. Fenton system. Figures 7a and 7b show the percentages of color and TOC removals of all Cu-iAlpill-MMTs in the presence of H_2O_2, respectively. It was found that the percentages of color and TOC removals gradually increased as reaction time and Cu^{2+}amount used in the impregnation process increased. The Cu-iAlpill-MMT-13wt% exhibited the highest ability for RO16 removal even though it possessed the lowest pore volume, suggesting that the Cu-iAlpill-MMTs tend to act more as the heterogeneous catalysts for the degradation of RO16 molecules than the simple adsorbents. The catalytic degradation of RO16 was considered to be initiated by the Cu^{2+}ions leached out from the CuO in both interior pores and surfaces of the Cu-iAlpill-MMTs. The Cu^{2+}ions could promote the decomposition of H_2O_2 to strong oxidizing species, i.e. hydroperoxyl radical (HOO•) and hydroxyl (HO•) as reported elsewhere [20–22]. These reactive radicals could oxidize the RO16 molecules, causing the cleavages of azo linkage (–N = N–), C–S bond between the aromatic ring and sulfonate group, C–N bond between the naphthalene ring and azo group and aromatic ring opening [23]. These oxidation reactions resulted in the decolorization of RO16 due to the degradation of chromophore and auxochrome, which are responsible for their color. In addition, the cleavage fragments of oxidized RO16 were considered to be mineralized by the reactive radicals as evidently observed in the significant increase of TOC removal.

Table 2
Percentages of color and TOC removals of Cu-iAlpill-MMTs in the Fenton (Cu-iAlpill-MMTs/H_2O_2) and photo-Fenton systems (Cu-iAlpill-MMTs/H_2O_2/UV)

Systems	Color removal (%)						TOC removal (%)					
	Reaction time (min)						Reaction time (min)					
	30	60	90	120	240	360	30	60	90	120	240	360
Cu–iAlpill–MMT–4wt%/H_2O_2	–	54	–	68	80	88	–	36	–	52	75	81
Cu–iAlpill–MMT–4wt%/H_2O_2/UV	44	63	69	75	86	89	35	48	56	65	80	81
Cu–iAlpill–MMT–7wt%/H_2O_2	–	61	–	77	89	94	–	45	–	64	85	93
Cu–iAlpill–MMT–7wt%/H_2O_2/UV	74	82	91	94	97	98	67	80	89	91	93	95
Cu–iAlpill–MMT–10wt%/H_2O_2	–	70	–	83	94	99	–	56	–	74	88	96
Cu–iAlpill–MMT–10wt%/H_2O_2/UV	98	99	100	100	100	100	93	99	98	100	100	100
Cu–iAlpill–MMT–13wt%/H_2O_2	–	73	–	85	95	99	–	58	–	74	88	97
Cu–iAlpill–MMT–13wt%/H_2O_2/UV	98	100	100	100	100	100	95	99	100	100	100	100

B. Photo-Fenton system. Figures 8a and 8b show the percentages of color and TOC removals of all Cu-iAlpill-MMTs in the presence of H_2O_2 and UV radiation, respectively. Under the UV radiation, all Cu-iAlpill-MMT catalysts exhibit significantly higher color and TOC removals than those performed without UV radiation using the same reaction time. These results were attributed to the synergistic effect of UV radiation and Cu^{2+}ions leached from the Cu-iAlpill-MMTs on the rapid degradation of H_2O_2 and H_2O into the HO• radicals, bringing about the faster decolorization and mineralization of RO16 molecules. The systems with the higher Cu content in the Cu-iAlpill-MMTs and/or the longer reaction time exhibited the higher percentages of colour and TOC removals. However, the efficiency of RO16 removal of Cu-iAlpill-MMT-10wt% was quite close to that of Cu-iAlpill-MMT-13wt%, although the Cu content in the Cu-iAlpill-MMT-10wt% was lower than that in the Cu-iAlpill-MMT-13wt%. This result was considered to be caused by the fact that the excess Cu in the Cu-iAlpill-MMT-13wt% which formed as CuO clusters on its exterior surface might partially hinder the migration of Cu^{2+}ions leached from the interior. It was, therefore, both Cu-iAlpill-MMT-10wt% and Cu-iAlpill-MMT-13wt% could completely eliminate the RO16 within 60 min when using the photo-Fenton systems.

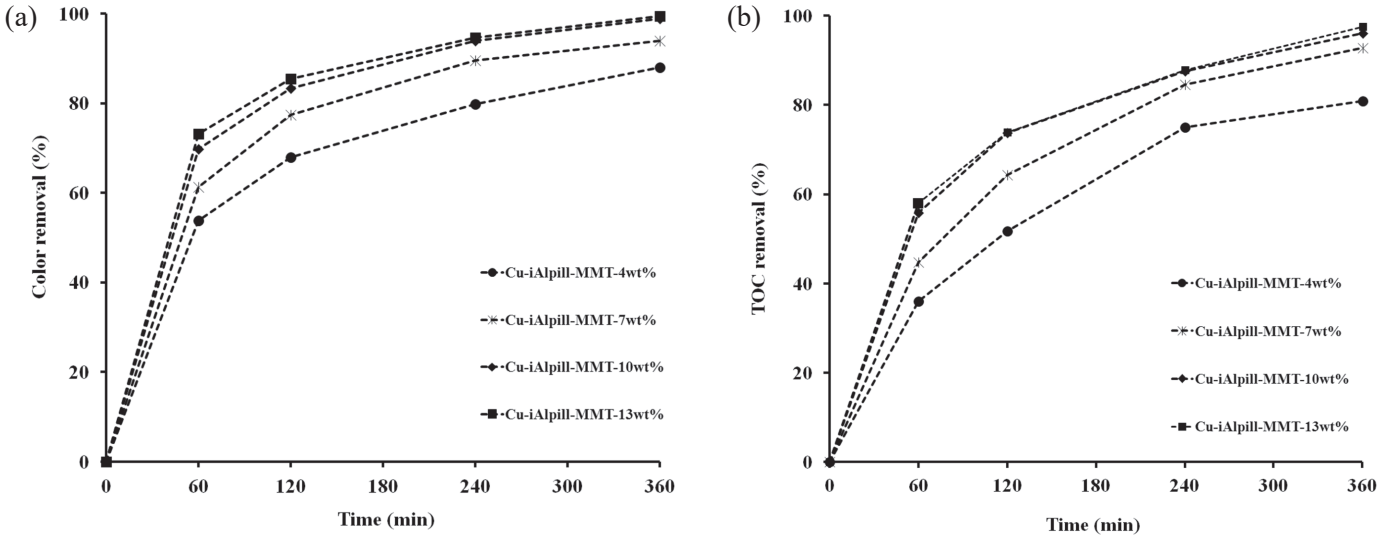

Fig. 7. Efficiencies of Cu-iAlpill-MMTs for (a) colour and (b) TOC removals in Fenton systems

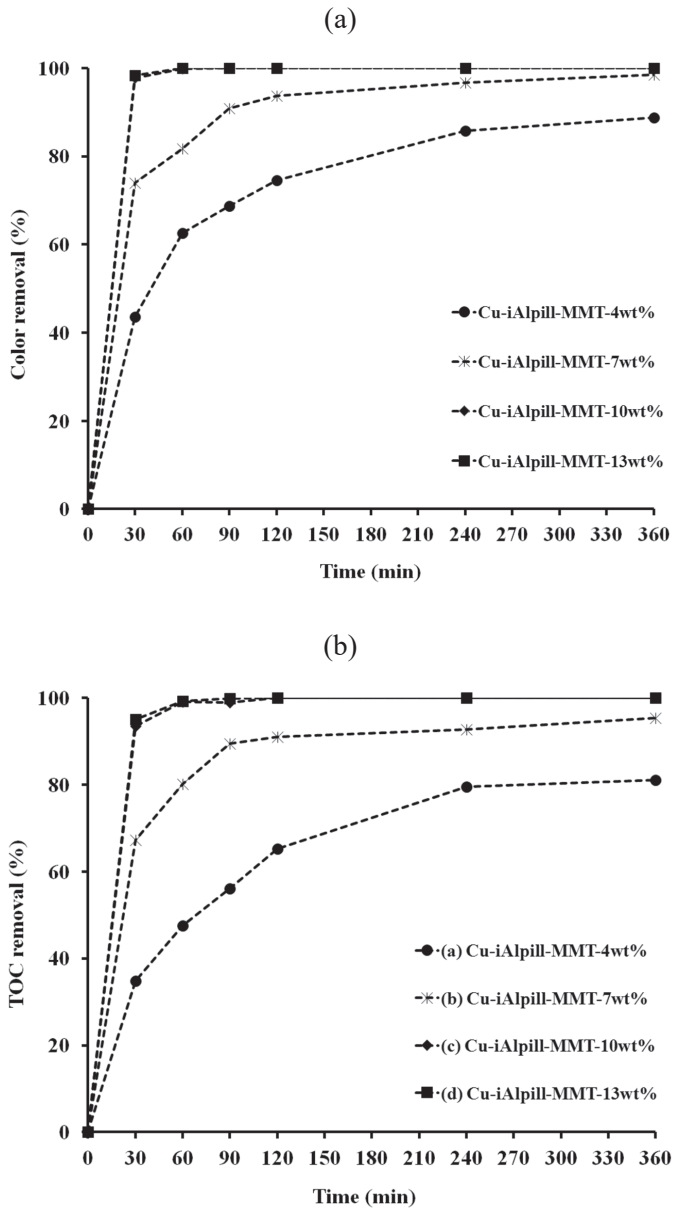

Fig. 8. Efficiencies of Cu-iAlpill-MMTs for (a) colour and (b) TOC removals in photo-Fenton systems

4. Conclusions

Copper impregnated aluminum pillared montmorillonites (Cu-iAlpill-MMTs) were successfully prepared by direct impregnation of $CuSO_4 \cdot 5H_2O$ aqueous solution into the precursor of aluminum polyohydroxy cation montmorillonite (AlOH-MMT). The impregnated Cu was calcined to CuO crystalline phase which occupied not only the interior interlayers but also the exterior surfaces of aluminum pillared montmorillonites. The slit-liked mesopore structures were obtained in the Cu-iAlpill-MMTs, in which the specific surface area and pore volume of Cu-iAlpill-MMTs were slightly decreased when copper loading increased. The Cu-iAlpill-MMTs with CuO rich surfaces could inhibit the growth of *E. coli*, indicating their antibacterial activities. In addition, the as-prepared Cu-iAlpill-MMTs could act as heterogeneous catalysts for decolorization and mineralization of reactive orange 16 (RO16) when applying them in the Fenton (Cu-iAlpill-MMT/H_2O_2) and photo-Fenton (Cu-iAlpill-MMT/H_2O_2/UV) treatment systems. The percentages of color and TOC removals gradually increased with the increases of the Cu content in the Cu-iAlpill-MMTs and the treatment times used in the Fenton and photo-Fenton systems. The decolorization and mineralization of RO16 in the Fenton system was faster than those in the photo-Fenton system. The Cu-iAlpill-MMT-13wt% showed the highest and color and TOC removals in both Fenton and photo Fenton systems.

Acknowledgments. The authors would like to acknowledge the financial support from Thai governmental budget for fiscal year 2015.

References

[1] J. Bovey, F. Kooli, and W. Jones, "Preparation and characterization of Ti-pillared acid-activated clay", *Clays. Miner.* 31, 501–506 (1996).

[2] J.T. Kloprogge, "Synthesis of smectites and porous pillared clay catalysts: review", *J. Porous. Mater.* 5, 5–41 (1998).

[3] P. Yuan, H. He, F. Bergaya, D. Wu, Q. Zhou, and J. Zhu, "Synthesis and characterization of delaminated iron-pillared clay with meso-microporous structure", *Microporous. Mesoporous. Mater*. 88, 8–15 (2006).

[4] H. Guo, X. Jing, L. Zhang, and J. Wang, "Preparation of inorganic-organic pillared montmorillonite using ultrasonic treatment", *J. Mater. Sci*. 42, 6951–6955 (2007).

[5] P. Tepmatee and P. Siriphannon, "Effect of Preparation Method on Structure and Adsorption Capacity of Aluminium Pillared Montmorillonite", *Mater. Res. Bull*. 48, 4856–4866 (2013).

[6] K. Pirkanniemi and M. Sillanpaa, "Heterogeneous water phase catalysis as an environmental application: a review", *Chemosphere* 48, 1047–1060 (2002).

[7] M.A. Vicente, C. Belver, R. Trujillano, M.A. Bañares-Muñoz, V. Rives, S.A. Korili, A. Gil, L.M. Gand´ıa, and J.F. Lambert, "Preparation and characterisation of vanadium catalysts supported over alumina-pillared clays", *Catal. Today*. 78, 181–190 (2003).

[8] E.G. Garrido-Ramírez, B.K.G. Theng, and M.L. Mora, "Clays and oxide minerals as catalysts and nanocatalysts in Fenton-like reactions-A review", *Appl. Clay. Sci*. 47, 182–192 (2010).

[9] F. Nerud, P. Baldian, J. Gabriel, and D. Ogbeifun, "Decolorization of synthetic dyes by the Fenton reagent and the Cu/pyridine/H_2O_2 system", Chemosphere 44, 957–961 (2001).

[10] J.K. Kim, F. Martinez, and I.S. Metcalfe, "The beneficial role of use of ultrasound in heterogeneous Fenton-like system over supported copper catalysts for degradation of *p*-chlorophenol", *Catal. Today*. 124, 224–231 (2007).

[11] S. Xia, L. Hui, Z. Yaobin, Z. Yazhi, and Q. Xie, "Efects of Cu(II) and humic acid on atrazine photodegradation", *J. Environ. Sci.* 23(5), 773–777 (2011).

[12] S. Zhou, Z. Qian, T. Sun, J. Xu, and C. Xia, "Catalytic wet peroxide oxidation of phenol over Cu–Ni–Al hydrotalcite", *Appl. Clay. Sci*. 53, 627–633 (2011).

[13] S. Caudo, G. Centi, C. Genovese, and S. Perathoner, "Copper and iron-pillared clay catalysts for the WHPCO of model and real wastewater streams from olive oil milling production", *Appl. Catal. B- Environ*. 70, 437–446 (2007).
[14] S. Caudo, C. Genovese, S. Perathoner, and G. Centi, "Copper-pillared clays (Cu-PILC) for agro-food wastewater purification with H_2O_2", *Microporous. Mesoporous. Mater.* 107, 46–57 (2008).
[15] P. Majzlik, A. Strasky, V. Adam, M. Nemec, L. Trnkova, J. Zehnalek, J. Hubalek, I. Provaznik, and R. Kizek, "Influence of zinc(II) and copper(II) ions on streptomyces bacteria revealed by electrochemistry", *Int. J. Electrochem. Sci*. 6, 2171–2191 (2011).
[16] C. Yu-Hao, H. Chung-Fang, O. Keng-Liang, and P. Pei-Wen, "Mechanical properties and antibacterial activity of copper doped diamond-like carbon films", *Surf. Coat. Technol*. 206, 1037–1040 (2011).
[17] P. Tepmatee and P. Siriphannon, "Nanoporous copper doped aluminium pillared montmorillonite for dye-containing wastewater treatment", *Water. Environ. Res*. doi: 10.2175/106143015X14362865227076 (2015).
[18] R.B. Chavan, "Environment-friendly dyeing processes for cotton", *Indian. J. Fibre. Text.* 26, 93–100 (2001).
[19] M.S. Hassan, T. Amna, O-B. Yang, M.H. El-Newehy, S.S. Al-Deyab, and M-S. Khil, "Smart copper oxide nanocrystals: Synthesis, characterization, electrochemical and potent antibacterial activity", *Colloids. Surf. B.* 97, 201–206 (2012).
[20] F. Haber and J. Weiss, "The catalytic decomposition of hydrogen peroxide by iron salts", *J. Proc. Roy. Soc. London. A*. 147, 332–351 (1934).
[21] M.N. Timofeeva, S.Ts. Khankhasaeva, E.P. Talsi, V.N. Panchenko, A.V. Golovin, E.Ts. Dashinamzhilova, and S.V. Tsybulya, "The effect of Fe/Cu ratio in the synthesis of mixed Fe, Cu, Al-clays used as catalysts in phenol peroxide oxidation", *Appl. Catal. B: Environ*. 90, 618–627 (2009).
[22] F.V.F Araujo, L. Yokoyama, L.A.C. Teixeira, and J.C. Campos, "Heterogeneous Fenton process using the mineral hematite for the discolouration of a reactive dye solution", Braz. J. Chem. Eng. 28, 605–616 (2011).
[23] S.S. Kumar, T. Muruganandham, and M.S.M. Jaabir, "Decolourization of Azo dyes in a two-stage process using novel isolate and advanced oxidation with Hydrogen peroxide / HRP system", *Int. J. Curr. Microbiol. App. Sci*. 3, 514–522 (2014).